DMAPT-D6 induces death-receptor-mediated apoptosis to inhibit glioblastoma cell oncogenesis via induction of DNA damage through accumulation of intracellular ROS

YA-JUN ZHANG, DONG-LIN YANG, HONG-XIA QIN, LIU-JUN HE, JIU-HONG HUANG, DIAN-YONG TANG, ZHI-GANG XU, ZHONG-ZHU CHEN and YONG LI

College of Pharmacy, National and Local Joint Engineering Research Center of Targeted and Innovative Therapeutics, Chongqing Key Laboratory of Kinase Modulators as Innovative Medicine, Chongqing University of Arts and Sciences, Chongqing 402160, P.R. China

Received June 22, 2020; Accepted December 7, 2020

DOI: 10.3892/or.2021.7932

Abstract. Glioblastoma (GBM) is an aggressive malignancy with a high rate of tumor recurrence after treatment with conventional therapies. Parthenolide (PTL), a sesquiterpene lactone extracted from the herb *Tanacetum parthenium* or feverfew, possesses anticancer properties against a wide variety of solid tumors. In the present study, a series of PTL derivatives were synthesized and screened. An inhibitor, dimethylaminoparthenolide (DMAPT)-D6, a derivative of the PTL prodrug DMAPT in which the hydrogen of the dimethylamino group is substituted for the isotope deuterium, induced significant cytotoxicity in GBM cells *in vitro* and induced cell cycle arrest at the S-phase in a dose-dependent manner. Furthermore, mechanistic investigation indicated that through increasing the levels of intracellular accumulation of reactive oxygen species (ROS), DMAPT-D6 triggered DNA damage and finally death receptor-mediated extrinsic apoptosis in GBM cells, suggesting that DNA damage induced by DMAPT-D6 initiated caspase-dependent apoptosis to remove damaged GBM cells. Taken together, these data suggested that ROS accumulation following treatment with DMAPT-D6 results in DNA damage, and thus, death-receptor-mediated apoptosis, highlighting the potential of DMAPT-D6 as a novel therapeutic agent for the treatment of GBM.

Correspondence to: Dr Dong-Lin Yang or Dr Yong Li, College of Pharmacy, National and Local Joint Engineering Research Center of Targeted and Innovative Therapeutics, Chongqing Key Laboratory of Kinase Modulators as Innovative Medicine, Chongqing University of Arts and Sciences, 319 Honghe Avenue, Yongchuan, Chongqing 402160, P.R. China
E-mail: dlyang@cqwu.edu.cn
E-mail: 18708168370@163.com

Key words: DMAPT-D6, glioblastoma, cell cycle, apoptosis, reactive oxygen species, DNA damage

Introduction

Glioblastoma (GBM) is the most aggressive primary intracranial malignancy of the central nervous system, and is often lethal (1-3). Currently, gliomas are classified into four grades (I-IV) by the World Health Organization according to their prognostic histopathological characteristics, of which, grade IV GBM is the most lethal (4). Despite significant advances in GBM research and treatment strategies including surgery, adjuvant postoperative radiotherapy and chemotherapy, the 5-year survival rate of glioma patients remains <5% after diagnosis (5). Therefore, novel treatment regimens, such as the development of novel drugs that target proliferating tumor cells, are required to prolong the survival of patients with brain tumors, particularly those with GBM.

Reactive oxygen species (ROS) are a group of short-lived, highly reactive, oxygen-containing byproducts of aerobic metabolism, including superoxide, hydroxyl radical, and hydroxides (6,7). Cellular ROS are primarily produced by mitochondria, NADPH oxidase, peroxisomes and in the endoplasmic reticulum (8-10). Emerging data have demonstrated that ROS serve as a double-edged sword in cellular processes (11). Low levels of ROS are required for cellular survival and proliferation (12,13). However, excessive ROS results in oxidative stress, resulting in DNA damage, apoptosis, and necrosis (14,15). DNA damage, induced by chemical and physical factors, is capable of initiating a series of processes, including cell cycle arrest, DNA repair, regulation of cell checkpoints and initiation of apoptosis (16). Increasing cellular ROS production, to induce DNA damage and cell death is a well-known effective anticancer strategy.

Parthenolide (PTL), a sesquiterpene lactone isolated from the shoots of *Tanacetum parthenium* (feverfew), has attracted increased attention owing to its antitumor activities in various human cancer cell lines (17). PTL induces cytotoxicity in a wide variety of solid tumors, including colorectal cancer, melanoma, pancreatic cancer, breast cancer, prostate cancer and GBM (18-27), but does not exert a notable effect on normal tissues (28). Although PTL possesses potency *in vitro*, lack of stability under both acidic and basic conditions as well as in

media containing 0.5% serum and its poor solubility are the major limitations for preventing its pharmacological applications (29-31). Moreover, the detailed mechanism of how PTL suppresses GBM growth still has not been fully elucidated. In particular, the effect on DNA damage and cell death induced by ROS has not been reported yet in GBM.

The aim of the present study was to synthesize PTL derivatives by improving its solubility for potential future medical use. DMAPT-D6, a derivative of dimethylaminoparthenolide (DMAPT), was shown to suppress the growth of GBM cells by inducing DNA damage initiated by excessive ROS accumulation. Moreover, mechanism analysis demonstrated that the DNA damage induced by DMAPT-D6 further induced cell cycle arrest at the S-phase and cell death receptor-mediated extrinsic apoptosis, suggesting that DMAPT-D6 is a promising anticancer agent, which increases ROS levels, resulting in the death of cancer cells.

Materials and methods

Reagents and antibodies. The derivatives of PTL were dissolved in DMSO (Thermo Fisher Scientific, Inc.) to obtain a stock solution of 40 mM, followed by further dilution with culture medium at various concentrations. Cells were treated with the compounds at the designated concentrations for 48 h, and DMSO was used as the vehicle. Penicillin-streptomycin, MTT and propidium iodide (PI) were purchased from Sigma-Aldrich; Merck KGaA. DMEM was purchased from HyClone (Cytiva) and FBS was purchased from Gibco (Thermo Fisher Scientific, Inc.). Z-DEVD-FMK was purchased from Topscience, and Z-IETD-FMK and N-acetylcysteine (NAC) were purchased from MedChemExpress. All the primary antibodies used in the present study were purchased from Cell Signaling Technology, Inc.: Anti-P27 (cat. no. 3686S, 1:1,000), anti-CDK1 (cat. no. 9116S, 1:1,000), anti-CDK2 (cat. no. 2546S, 1:1,000), anti-cyclin B1 (cat. no. 4138S, 1:1,000), anti-cyclin E1 (cat. no. 20808S, 1:1,000), anti-β-actin (cat. no. 4970S, 1:1,000), anti-nuclear factor-like 2 (NRF2; cat. no. 12721S, 1:1,000), anti-λH2AX (cat. no. 9718S, 1:1,000), anti-p53-binding protein 1 (53BP1; cat. no. 88439S, 1:1,000), anti-DNA Ligase IV (cat. no. 14649S, 1:1,000), anti-DR3 (cat. no. 45901S, 1:1,000), anti-DR5 (cat. no. 3696S, 1:1,000), anti-FADD (cat. no. 2782S, 1:1,000), anti-TRADD (cat. no. 364S, 1:1,000), anti-cleaved caspase-8 (cat. no. 9496S, 1:1,000), anti-PARP (cat. no. 9532S, 1:1,000), anti-caspase-3 (cat. no. 9662S, 1:1,000) and anti-cleaved caspase-3 (cat. no. 9664S, 1:1,000). The secondary antibodies used for western blotting were IRDye® 680RD donkey anti-mouse IgG secondary antibody (cat. no. 926-68072, 1:15,000) and IRDye® 800CW donkey anti-rabbit IgG secondary antibody (cat. no. 926-32213, 1:15,000), and were purchased from LI-COR Biosciences. The secondary antibodies: anti-rabbit IgG (H + L) ReadyProbes™ secondary antibody, Alexa Fluor 488 (cat. no. R37118, 1:2,000), used for immunofluorescence, were purchased from Thermo Fisher Scientific, Inc.

Cell lines and culture. Human glioblastoma cell lines U87 and LN229 were obtained from Cobioer, and both cell lines were free of mycoplasma and were authenticated using STR detection. The origin of glioblastoma cell line U87 (ATCC® HTB-14™) used in the present study was unknown as this cell line was originally obtained from American Type Culture Collection. Cells were cultured in high-glucose DMEM supplemented with 10% FBS, 1% penicillin-streptomycin at 37˚C in a humidified incubator with 5% CO_2.

Cell viability assay. U87 and LN229 cells were plated in 96-well plates ($3x10^3$ cells/well) and incubated overnight at 37˚C. After treatment with various concentrations of test compounds for designed times, MTT solution was added (20 μl/well), and the plates were incubated for an additional 4 h. Next, the supernatant medium was removed and the crystals were solubilized in DMSO (200 μl/well). A microplate reader (Bio-Tek Instruments, Inc.) was used to detect the absorbance value at 570 nm. All experiments were performed in triplicate, independently.

Colony formation assay. A total of $1x10^3$ cells/well were seeded in 6-well plates, respectively, and allowed to culture overnight prior to treatment. After exposure to the designated concentrations of DMAPT-D6 for 48 h, the cells were cultured with fresh DMEM for another 15 days. Following fixation at 4˚C with 4% paraformaldehyde solution for 30 min, the cells were stained with 1% crystal violet at room temperature for 30 min to visualize colonies. The number of colonies with ≥50 cells was counted under a scanner.

Western blotting. The harvested glioma cells were lysed in RIPA lysis buffer (Beyotime Institute of Biotechnology) supplemented with Halt™ Protease and Phosphatase Inhibitor Cocktail (Thermo Fisher Scientific, Inc.) at 4˚C for 30 min. After quantification of total protein concentration using a BCA Protein assay kit (Beyotime Institute of Biotechnology), protein samples (30 μg/lane) were loaded on 8, 10 and 12% SDS gels, resolved by electrophoresis and transferred to PVDF membranes (Millipore). Subsequently, the membranes were blocked with 5% BSA in TBST for 2 h at room temperature, and then incubated with the indicated primary antibodies overnight at 4˚C. Following incubation with the corresponding IRDye 800CW donkey anti-mouse IgG (H + L) or IRDye 680LT donkey anti-rabbit IgG (H + L) secondary antibody, immunoreactivity was visualized using an odyssey two-color infrared fluorescence imaging system (LI-COR Biosciences). β-actin was used as the loading control.

Flow cytometry analysis. Glioma cells in the logarithmic growth phase were harvested and transferred into 6-well plates at an estimated confluence of 30% per well. After pretreatment with NAC (5 mM) for 2 h, the cells were exposed to the different concentrations of DMAPT-D6 for 48 h. Additionally, other cells were treated with or without DMAPT-D6, Z-VAD-FMK, Z-IETD-FMK, DMAPT-D6 and Z-VAD-FMK or DMAPT-D6 and Z-IETD-FMK treatment. Then, all treated cells were collected and analyzed using flow cytometry analysis. For cell cycle analysis, the harvested cells were fixed with 70% ethanol at 4˚C for 24 h, and then washed three times with PBS. Subsequently, cells were incubated with PBS containing 50 mg/ml PI (BD Biosciences) and 100 mg/ml RNase (Sigma-Aldrich; Merck KGaA) at 37˚C for 30 min. Finally, the stained cells were analyzed using a BD Accuri™

C6 flow cytometry (BD Biosciences), and the results were statistically compared and automatically visualized using FlowJo 7.6 (FlowJo LLC). For cell apoptosis analysis, cells were harvested and stained with an Annexin V-FITC/PI apoptosis assay kit according to the manufacturer's protocol (BD Biosciences). The fluorescence-positive cells were analyzed using a flow cytometer within 1 h to assess the proportion of apoptotic cells, and the apoptotic rate was visualized using FlowJo.

Immunofluorescence. Glioma cells were grown on cover slips in 24-well plates prior to treatment with DMAPT-D6 for 48 h. After washing three times with PBS, cells were fixed in 4% paraformaldehyde at 4˚C for 30 min, permeabilized using 0.1% Triton X-100 for 10 min, and blocked in Immunol staining blocking buffer (Beyotime Institute of Biotechnology) for 30 min at 37˚C. Cells were then incubated overnight at 4˚C with anti-γH2AX (1:250) antibody. Subsequently, the stained cells were washed three times with PBS and incubated with Alexa Fluor-conjugated secondary antibodies (1:2,000) for 1 h at room temperature. For EdU cell proliferation staining, U87 and LN229 cells were stained using BeyoClick™ EdU Cell Proliferation kit with Alexa Fluor 594 according to the manufacturer's protocol (cat. no. C0078S; Beyotime Institute of Biotechnology). Then, 1 mg/ml DAPI was used to label nuclei for 30 min. Images were captured using a fluorescence microscope (Olympus IX53/DP80; Olympus Corp.).

Determination of ROS formation. ROS formation was detected using a ROS assay kit (Beyotime Institute of Biotechnology) according to the manufacturer's protocol. Briefly, following pretreatment with or without NAC (5 mM) diluted in serum-free DMEM for 2 h, glioma cells were further treated with DMAPT-D6 for 48 h before staining with DCFH-DA (10 μM) for 30 min. Subsequently, cell suspensions were centrifuged and washed three times with serum-free DMEM, and then visualized using a fluorescence microscope (Olympus IX53/DP80; Olympus Corp.).

Statistical analysis. GraphPad Prism version 7.0 (GraphPad Software, Inc.) was used for the statistical analysis. Data are presented as the mean ± standard deviation, and the ANOVA method was used to compare differences between groups. $P<0.05$ was considered to indicate a statistically significant difference.

Results

Synthesis of PTL derivatives. The syntheses of the PTL derivatives was initiated using readily available PTL (Fig. 1). PTL was treated with *p*-toluenesulfonic acid (p-TSA) to obtain micheliolide (MCL) and then subjected to epoxidation with *m*-CPBA to obtain compound **1**. Then, this compound was subjected to elimination with $POCl_3$/pyridine to obtain arglabin. PTL, MCL, compound **1** and arglabin were treated with dimethylamine in tetrahydrofuran under base conditions to generate DMAPT, compound **2**, compound **3**, and compound **4**, respectively. Similarly, DMAPT-D6, compound **5**, compound **6** and compound **7** were obtained by treating PTL, MCL, compound 1 and arglabin with dimethyl-d6-amine under the same conditions. All compounds were characterized by ^{1}H NMR and ^{13}C NMR (Figs. S1-22) and the detailed synthesis process of the PTL derivatives is shown in Appendix S1.

Cytotoxic effect of DMAPT-D6 on GBM cells. Given the anticancer effects of PTL, whether the newly synthesized PTL-related derivatives could inhibit proliferation and growth of GBM cells was assessed. The effects of PTL-related derivatives on cell viability were determined (Table SI) and the IC_{50} values of DMAPT-D6 were 15.5 and 11.15 μM in the U87 and LN229 cells, respectively (Fig. 2A). To further examine the inhibitory effects of DMAPT-D6, GBM cells were treated with 2.5, 5, 10, 20 and 40 μM for 24, 48 and 72 h and the relationship between cell growth and concentration, as well as period of treatment were assessed. The cell growth curve showed that DMAPT-D6 reduced the proliferative ability of both U87 and LN229 cells in a dose- and time-dependent manner, highlighting the dose- and time-dependent cytotoxicity of this compound on GBM cells (Fig. 2B). A colony formation assay was performed to further confirm the growth-inhibitory effects of DMAPT-D6 on GBM cells. The results indicated that cells exposed to DMAPT-D6 exhibited a significantly reduced cell growth in a dose-dependent manner, as evidenced by the smaller colonies and decreased colony numbers compared with the control group (Fig. 2C). Consistently, in comparison with the untreated group, the number of EdU-positive cells was significantly decreased in a dose-dependent manner following exposure to DMAPT-D6, demonstrating its ability to suppress proliferation in U87 and LN229 cells (Fig. 3A).

DMAPT-D6 arrests cell cycle progression by arresting GBM cells at the S-phase. To determine the mechanism underlying cytotoxicity of the DMAPT-D6 in GBM cells, cell cycle analysis was performed on both U87 and LN229 cells treated with or without the inhibitor. Flow cytometry indicated that 5 μM DMAPT-D6 resulted in cell cycle arrest at the S-phase, whereas 20 μM DMAPT-D6 significantly induced arrest at S-phase by reducing the proportion of cells in the G0/G1 phase (Fig. 3B). Since the effect of DMAPT-D6 on cell cycle arrest in U87 and LN229 cells was determined, its effect on the expression levels of S-phase-related proteins was further examined to confirm the regulatory role in cell cycle distribution. As shown in Fig. 3C, immunoblotting showed that DMAPT-D6 considerably decreased the levels of cyclin B, cyclin E, cyclin-dependent kinase 1 (CDK1) and CDK2, whereas p27 expression was increased following exposure to DMAPT-D6 in a dose-dependent manner in U87 and LN229 cell lines. Taken together, these data suggest that DMAPT-D6 may suppress cell proliferation by inducing S-phase cell cycle arrest in GBM cells.

DMAPT-D6 induces DNA damage through excessive generation of ROS in GBM cells. To gain additional insight into the mode of DMAPT-D6-induced inhibition of proliferation, intracellular ROS generation was evaluated by fluorescence microcopy after incubation with the specific ROS-detecting fluorescent dye, DCFH-DA in U87 and LN229 cells. As indicated in Fig. 4A, ROS levels were significantly induced in response to different concentrations of DMAPT-D6

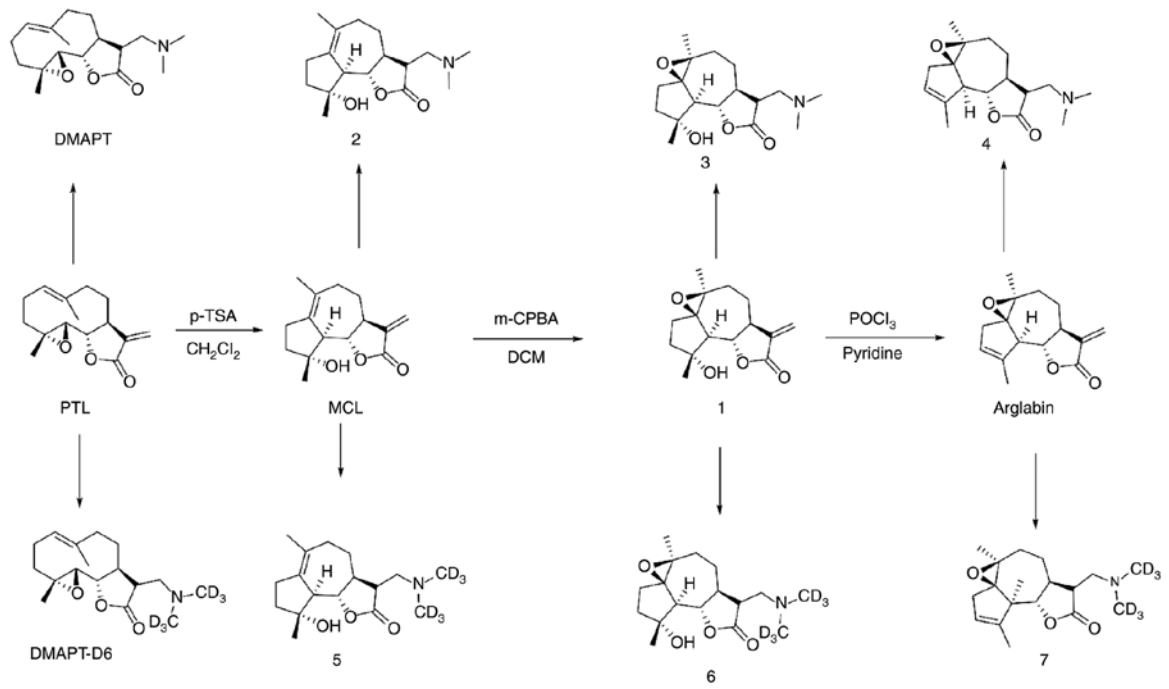

Figure 1. Strategy for synthesis of the parthenolide derivatives. DMAPT, dimethylaminoparthenolide; PTL, parthenolide; MCL, micheliolide; p-TSA, *p*-toluenesulfonic acid.

when compared with the control. Interestingly, the expression of the oxidative stress responsive gene, NRF2, was significantly upregulated after treatment with DMAPT-D6 in a dose-dependent manner, suggesting excessive ROS accumulation within cells and the initiation of the ROS stress response (Fig. 4C). It has been reported that accumulation of intracellular ROS could induce DNA damage and influence the DNA damage response caused by genotoxic therapy, particularly in the context of double-strand breaks (32). To evaluate whether DMAPT-D6 could initiate DNA damage through accumulation of excessive intracellular ROS, γH2AX, the phosphorylated of histone H2AX and a marker of DNA double-strand breaks, was detected in both U87 and LN229 cell lines using immunofluorescence and immunoblotting. As illustrated in Fig. 4B, the results showed that the green signal representing γH2AX significantly accumulated in the nuclei in a dose-dependent manner compared with the control group. Consistent with this, immunoblotting indicated that γH2AX was significantly upregulated in the presence of DMAPT-D6 in U87 and LN229 cells (Fig. 4C), suggesting that DNA double-strand breaks were generated in GBM cells in response to the treatment. Furthermore, expression of p53, 53BP1 and DNA ligase IV (LIG IV), which are both proteins involved in the DNA repair process, were significantly decreased in a dose-dependent manner, demonstrating DNA repair suppression in response to DMAPT-D6 (Fig. 4C).

Induction of ROS and DNA damage by DMAPT-D6 contributes to death receptor-mediated external-apoptosis in GBM cells. A disproportional increase in ROS and severe DNA damage can induce the intrinsic and extrinsic apoptotic pathways, which are mediated by mitochondria and cell death receptor signaling, respectively (33-37). Given the effects of DMAPT-D6 on the induction of ROS and subsequent DNA damage, whether apoptosis was initiated in response to DMAPT-D6 was assessed. Of note, the PI staining assay showed that the percentage of PI-positive cells was significantly increased following treatment with DMAPT-D6 in U87 and LN229 cells in a dose-dependent manner (Fig. 5A), indicating the induction of apoptosis. To further confirm the effects of DMAPT-D6 on apoptosis, an Annexin V-FITC/PI assay was performed using flow cytometry after U87 and LN229 cells were treated with the DMAPT-D6 (at 5, 10 and 20 μM) for 48 h. As shown in Fig. 5B, at a low dose of 5 μM, DMAPT-D6 induced 7.28 and 10.7% late-phase apoptosis (both Annexin-V and PI positive-cells) in U87 and LN229 cell lines, respectively. At a dose of 20 μM, the percentage of apoptosis rose to 73.2 and 52.7%, respectively. Subsequently, the expression of extrinsic apoptotic signaling-related proteins was assessed to determine whether the cell death receptor was involved in the apoptosis in response to DMAPT-D6 treatment. Consistently, cell death receptor signaling pathway-related proteins such as death receptor (DR)3, DR5, Fas-associated death domain (FADD) and tumor necrosis factor receptor-associated death domain (TRADD) were significantly upregulated in a dose-dependent manner after exposure to DMAPT-D6 (Fig. 5C). Subsequently, procaspase 8 was cleaved and the active enzyme form, caspase 8, was produced due to the increase in FADD and TRADD. Then, the downstream procaspase 3 and PARP were cleaved and activated in both U87 and LN229 cells after treatment with DMAPT-D6, suggesting that it primarily promotes extrinsic apoptosis by inducing death receptor-mediated apoptotic signaling (Fig. 5C).

To further confirm that DMAPT-D6 induced cell death receptor mediated-apoptosis, a pan-caspase inhibitor, Z-VAD-FMK, was used to detect the restorative effect on apoptosis caused by DMAPT-D6. As shown in Fig. 5D, Z-VAD-FMK

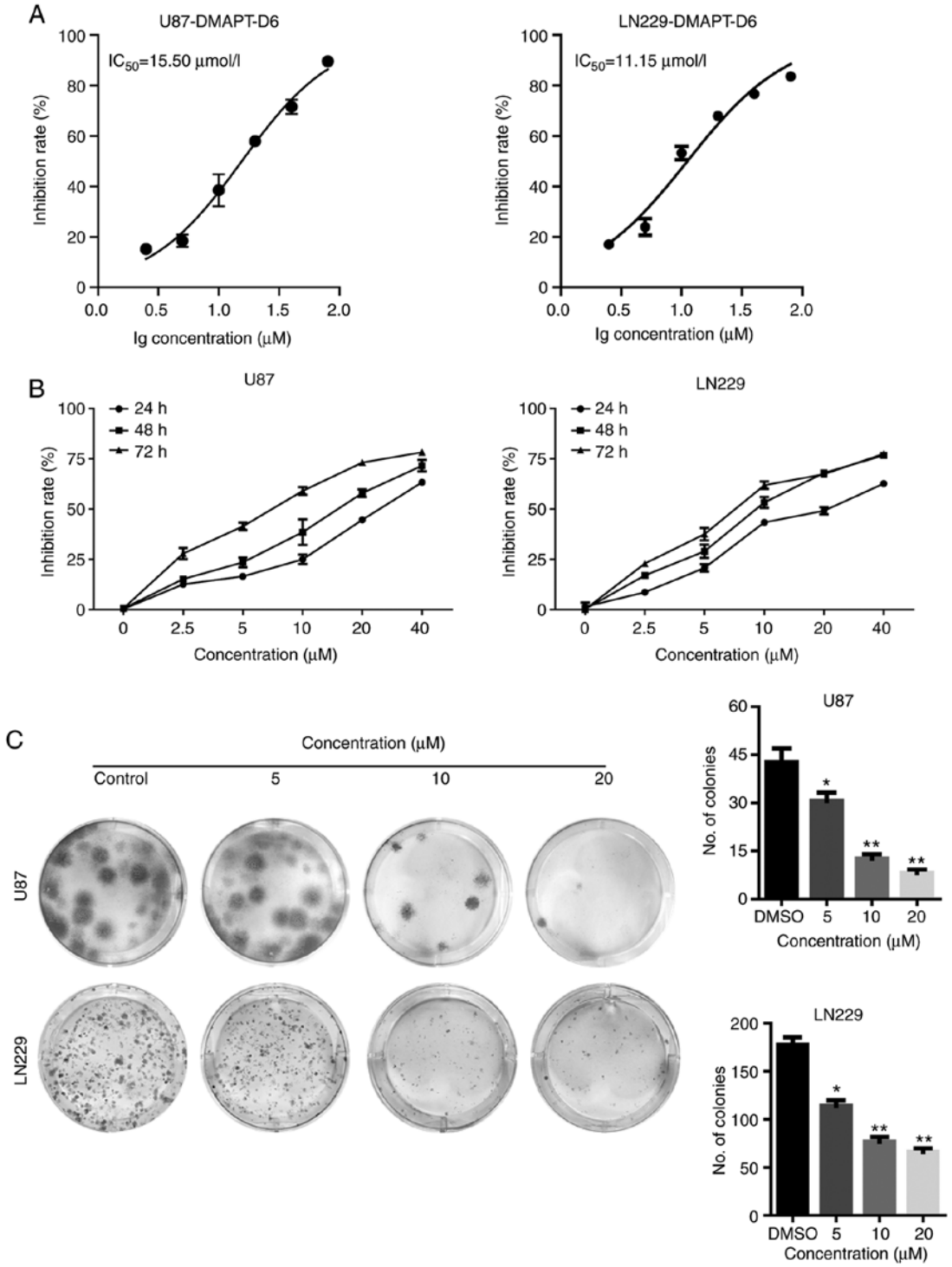

Figure 2. DMAPT-D6 suppresses proliferation and viability of GBM cells. (A) IC_{50} values of DMAPT-D6 in U87 and LN229 cells were calculated. (B) U87 and LN229 cells were treated with the indicated concentrations of DMAPT-D6 for 24, 48 and 72 h. Cell viability and growth were measured using an MTT assay. (C) A colony formation assay was used to assess *in vitro* growth of both U87 and LN229 cells following treatment with the indicated concentrations of DMAPT-D6 for 14 days. The colonies were visualized and quantified. Data are presented as the mean ± standard deviation of three independent experiments. *P<0.05, **P<0.01 vs. vehicle. DMAPT, dimethylaminoparthenolide; GBM, glioblastoma.

significantly rescued cell apoptosis induced by DMAPT-D6. Interestingly, Z-VAD-FMK also partially restored the protein levels of DNA repair protein DNA Lig IV, DR3, cleaved caspases-8 and -3, and PARP when treated with both reagents together (Fig. 5E). Furthermore, a specific inhibitor of caspase 8, Z-IETD-FMK, was used to examine the rescuing effect on death-receptor-mediated apoptosis induced by DMAPT-D6. The results showed that Z-IETD-FMK could partially reverse DMAPT-D6-induced apoptosis in both U87 and LN229 cell lines (Fig. 6A), demonstrating that caspase-dependent cell death was the primary cause of GBM cell death induced by DMAPT-D6.

A ROS scavenger, NAC, decreases the cytotoxicity of DMAPT-D6 in GBM cells. To further demonstrate whether

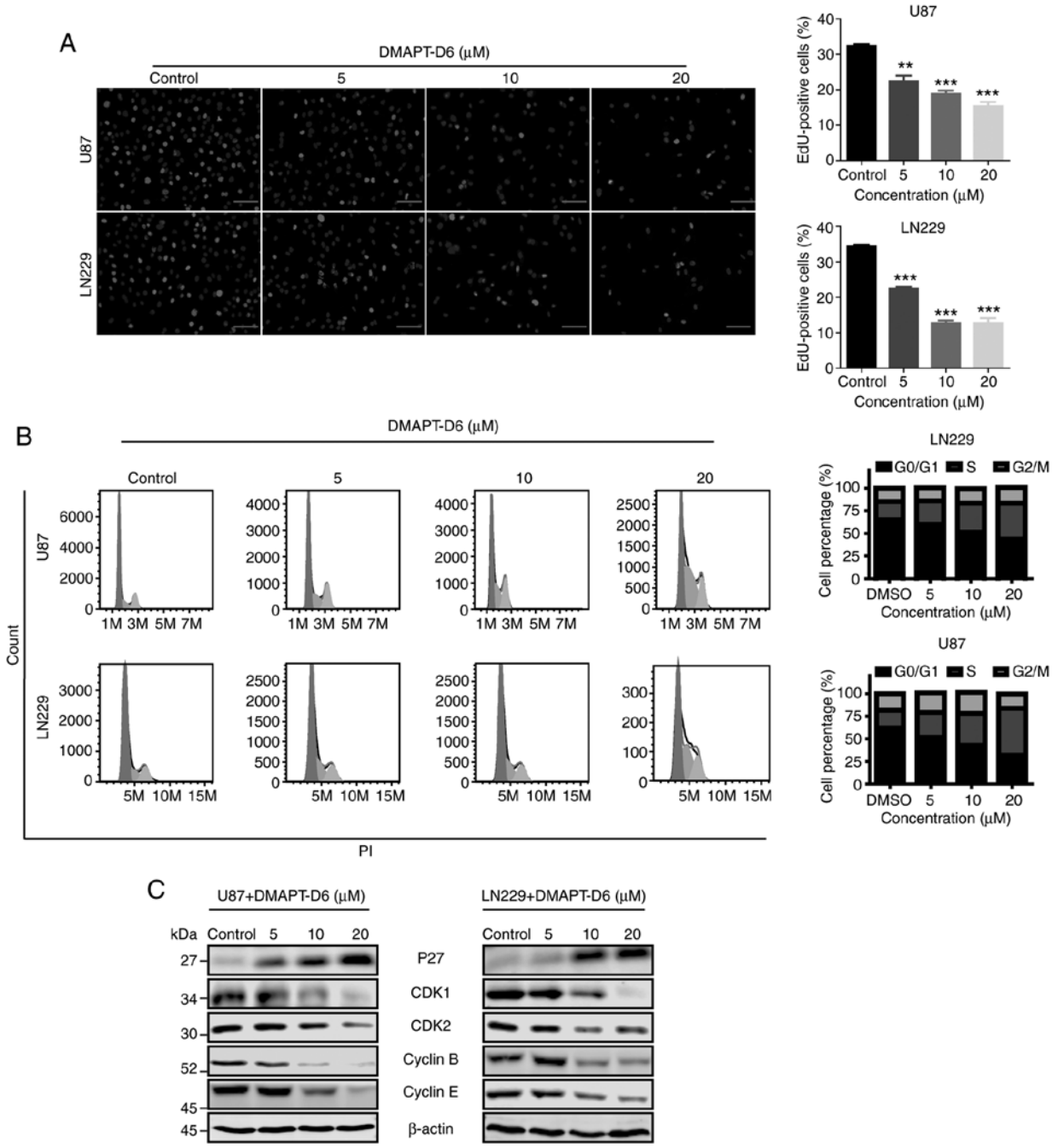

Figure 3. DMAPT-D6 induces cell cycle arrest at the S-phase in GBM cell lines. (A) EdU-staining assay was performed to further evaluate the inhibition of proliferation following treatment with DMAPT-D6 for 48 h. EdU-positive cells were counted. Scale bar, 100 μm. (B) Cell cycle analysis of U87 and LN229 cells was evaluated by flow cytometry in the presence of DMSO vehicle or DMAPT-D6. (C) Influence of DMAPT-D6 on expression levels of S-phase-related proteins. Expression levels of cyclin B, cyclin E, P27, CDK1 and CDK2 in U87 and LN229 cells were detected by western blotting. β-actin was used as the loading control. Data are presented as the mean ± standard deviation of three independent experiments. **P<0.01, ***P<0.001 vs. control. DMAPT, dimethylaminoparthenolide; GBM, glioblastoma; CDK, cyclin-dependent kinase.

the anticancer ability of DMAPT-D6 on GBM was actually initiated by generating excessive ROS, the effects of DMAPT-D6 on U87 and LN229 cells after treatment with an ROS scavenger, NAC, was determined. As expected, pretreating the cells with NAC significantly reduced the number of DCFH-DA-positive cells (Fig. 6B). NAC pretreatment improved the DMAPT-D6-mediated decrease in cell viability (Fig. 6C). Additionally, the effect of NAC on apoptosis induced by DMAPT-D6 was assessed. Flow cytometry showed that NAC could dramatically reduce the DMAPT-D6-mediated apoptotic cells (Fig. 6D). Subsequently, the essential effects of ROS on DMAPT-D6-induced DNA damage responses was examined after treatment with NAC. The results indicated that pretreating the cells with NAC significantly decreased the production of ROS and γH2AX, and upregulated the protein expression level involved in DNA damage response, such as 53BP1 and DNA LIG IV, suggesting causative involvement of ROS in DMAPT-D6-induced DNA damage (Fig. 6E). Collectively, these results showed that DMAPT-D6 induced apoptosis in GBM cells by resulting in the generation of excessive ROS,

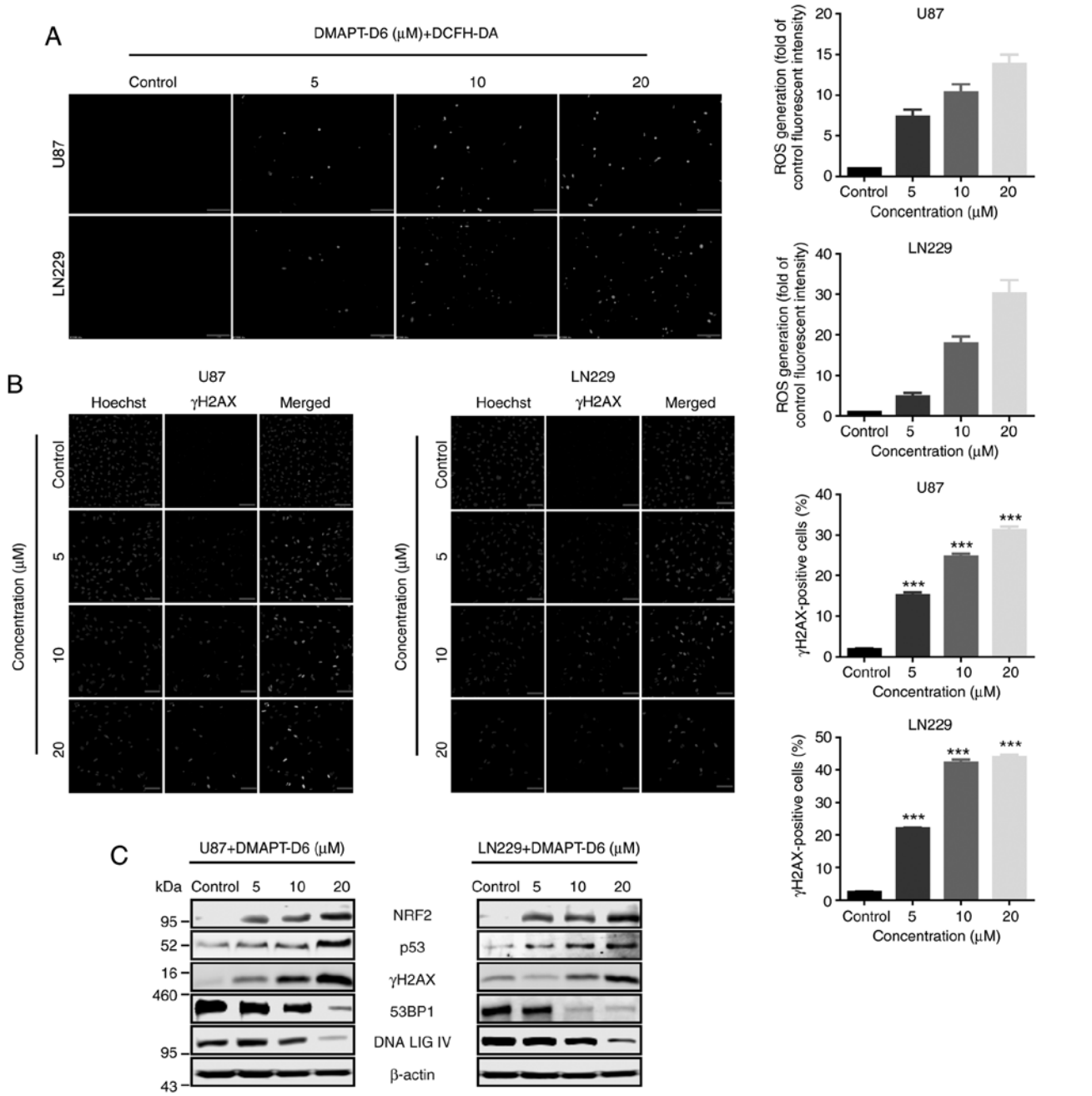

Figure 4. DMAPT-D6 induces accumulation of ROS and DNA damage, and impairs DNA repair. (A) GBM U87 and LN229 cells were treated with the indicated concentrations of DMAPT-D6 for 48 h, and then were exposed to DCFH-DA for another 30 min. Immunofluorescence analysis was performed to detect the green signal, indicative of ROS generation. Cells with a green signal were quantified. Scale bar, 100 μm. (B) γH2AX signal, the histone H2AX phosphorylation representing double-strand breaks, was detected using immunofluorescence, to assess the effects of DMAPT-D6 on DNA damage. γH2AX-positive cells were quantified. Scale bar, 100 μm. (C) Following treatment with different concentrations of DMAPT-D6, cells were lysed, and expression of γH2AX, oxidative stress response and DNA repair-related proteins, such as Nrf2, p53, 53BP1 and DNA ligase IV were examined by western blotting. β-actin was used as the loading control. Data are presented as the mean ± standard deviation of three independent experiments. ***P<0.001 vs. control. DMAPT, dimethylaminoparthenolide; GBM, glioblastoma; ROS, reactive oxygen species; LIG IV, ligase IV; NRF2, nuclear factor-like 2.

which acts as a trigger of downstream apoptotic pathways, such as DNA damage and caspase-dependent apoptosis.

Discussion

Although notable advances have been made in the treatment of glioblastoma (GBM), due to a high prevalence of development of resistance to radiotherapy and chemotherapy, patient prognosis remains poor (38,39). Thus, there is an urgent need to develop novel agents that can inhibit the proliferation and growth of GBM, and reverse acquisition of multidrug resistance in GBM cells. It has been reported that parthenolide (PTL) exhibits excellent anticancer, anti-inflammatory and other beneficial properties without cytotoxic effects on normal cells (17,40). Nevertheless, PTL has some disadvantages that prevent it from being developed as a clinical drug. For example, PTL is unstable under physiological conditions, and has

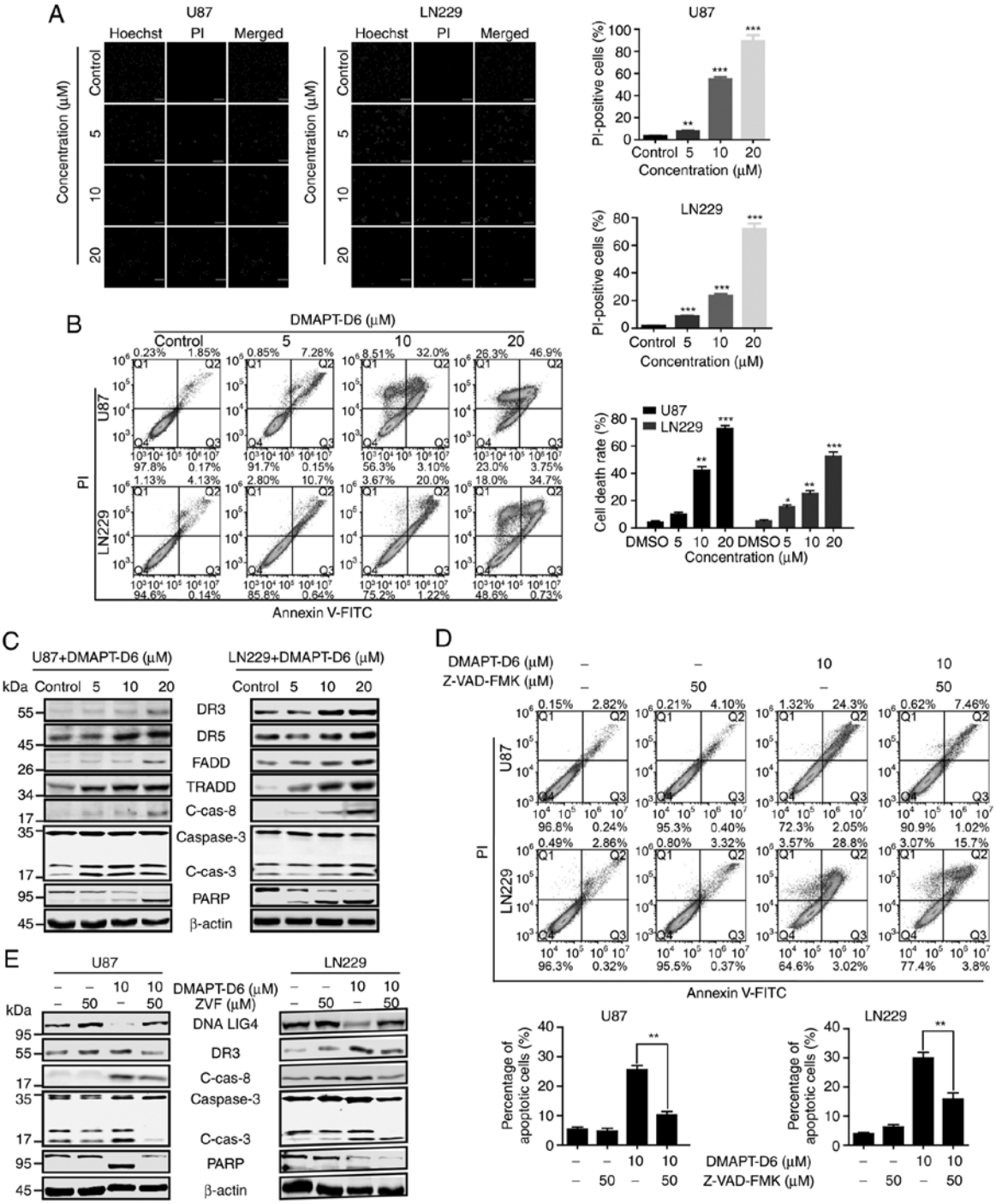

Figure 5. DMAPT-D6 promotes caspase-dependent death-receptor-mediated extrinsic apoptosis in both GBM U87 and LN229 cell lines. (A) PI-staining was performed to examine whether late apoptosis was induced after treatment with DMAPT-D6 in U87 and LN229 cells. Subsequently, cells were analyzed using immunofluorescence. (B) U87 and LN229 cells were treated with the indicated concentrations of DMAPT-D6 for 48 h. Subsequently, cells were harvested and stained with Annexin-V/PI. The Q4 (Annexin-V$^-$/PI$^-$), Q3 (Annexin-V$^+$/PI$^-$) and Q2 (Annexin-V$^+$/PI$^+$) quadrants represent the populations of normal, early apoptotic and late apoptotic cells, respectively. (C) Expression of death receptor-mediated extrinsic apoptosis-related proteins were detected using western blotting. (D) U87 and LN229 cells were treated with DMAPT-D6 (10 μM) either alone or combination with the apoptosis inhibitor Z-VAD-FMK (50 μM) for 48 h, and cells were stained with Annexin-V/PI to examine the recovery of apoptosis. (E) Expression of death receptor-mediated apoptosis-related proteins was examined using western blotting after treatment with DMAPT-D6 (10 μM) either alone or in combination with apoptosis inhibitor Z-VAD-FMK (ZVF) (50 μM). *P<0.05, **P<0.01, ***P<0.001 vs. control. DMAPT, dimethylaminoparthenolide; DR death receptor; FADD, Fas-associated death domain; TRADD, tumor necrosis factor receptor-associated death domain; PARP, poly(ADP-ribose) polymerase; C-Cas8, cleaved caspase-8; C-Cas3, cleaved caspase-3.

poor water solubility (29-31). Modifications of PTL have been reported to improve its activity, water solubility, stability and bioavailability. DMAPT, a prodrug formed by addition of dimethylamine to PTL, can improve its solubility and bioavailability (31,41,42). Interestingly, deuteration of existing drugs can further exhibit improved pharmacokinetic or toxicological properties, due to the stronger deuterium-carbon bond resulting in modified metabolism (31,42,43). Therefore, development of this approach and evaluation of the effects of deuterated

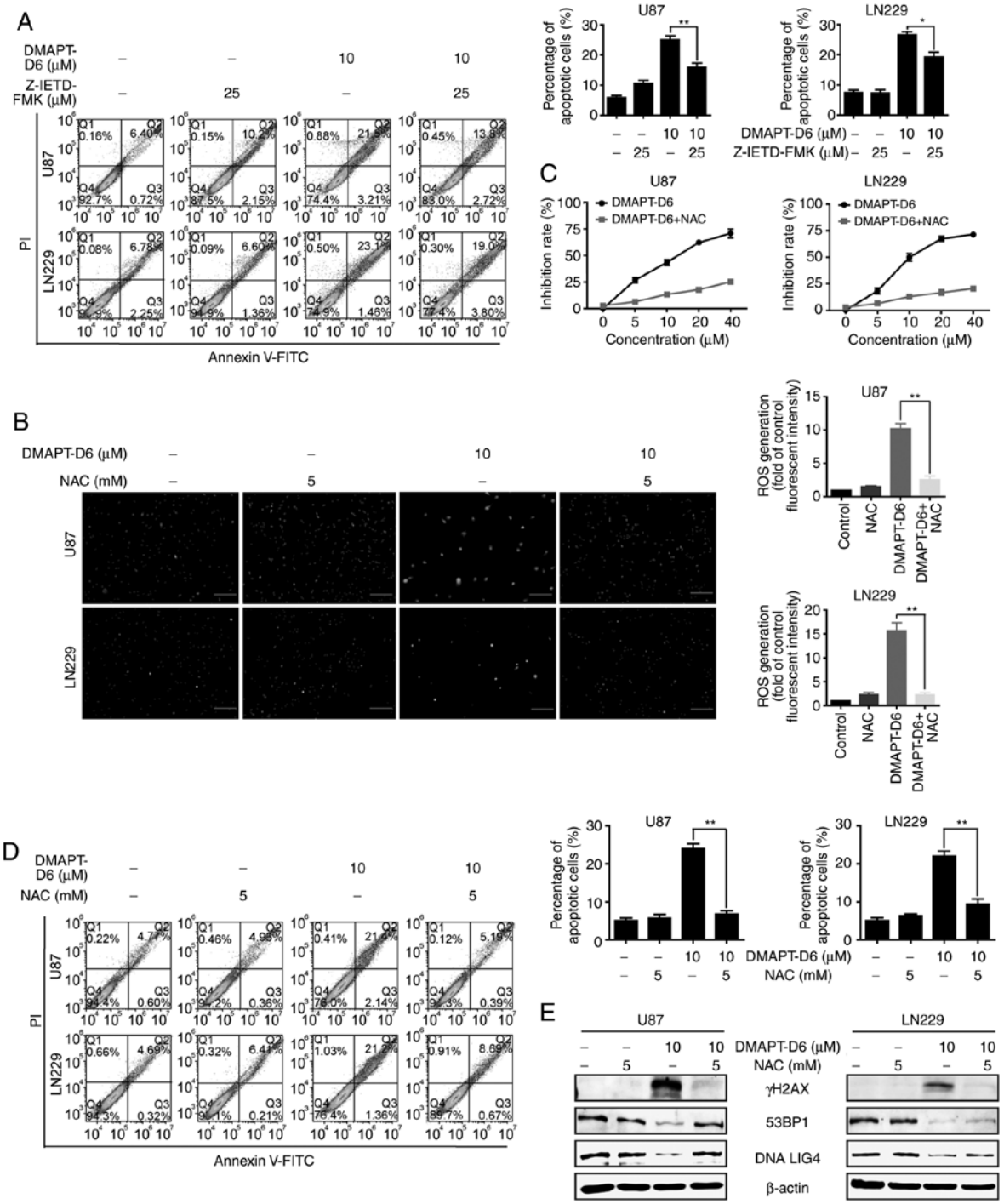

Figure 6. DMAPT-D6-induced cytotoxicity is dependent on intracellular ROS production in GBM cells. (A) The specific caspase-8 inhibitor, Z-IETD-FMK, partially decreased the apoptosis induced by DMAPT-D6. Both U87 and LN229 cell lines were treated with or without Z-IETD-FMK for 48 h before staining with PI and Annexin V. (B) NAC significantly reversed ROS production induced by DMAPT-D6. U87 and LN229 cells were treated with or without NAC (5 mM) for 2 h before staining with DCFH-DA for 30 min. Intracellular ROS was assessed by fluorescence microscopy. (C and D) Blocking of ROS generation decreased DMAPT-D6-mediated cytotoxicity and apoptosis. (E) Causative involvement of ROS in DMAPT-D6-induced DNA damage. Expression of proteins involved in DNA damage response was examined using western blotting following treatment with or without NAC. Data are presented as the mean ± standard deviation of three independent experiments. $^{*}P<0.05$, $^{**}P<0.01$ vs. control. DMAPT, dimethylaminoparthenolide; GBM, glioblastoma; NAC, N-acetylcysteine; LIG IV, ligase IV.

derivatives on cancer cells and its potential anticancer mechanisms are being intensively studied. In the present study, 12 PTL derivatives, including 4 deuterated compounds were synthesized and exhibited some extent of anti-proliferative activity against GBM cells. Among all of the synthesized compounds, DMAPT-D6 exhibited potent activity against both U87 and LN229 cell lines, prompting further exploration of its anti-proliferative effects, and the underlying molecular mechanism.

Despite ROS promoting the progression of cancer to some extent, when excessive accumulation of ROS reaches a certain threshold, this causes DNA damage, apoptosis and

necrosis (12-15). In the present study, the levels of intracellular ROS in both U87 and LN229 cells were measured after exposure to DMAPT-D6, and found that DMAPT-D6 significantly upregulated ROS levels in a dose-dependent manner. Therefore, these results suggested that the cells were under high oxidative stress. Recently, Carlisi *et al* (44) showed PTL downregulated Nrf2 expression in spheroids such as MDA-MB-232 and BT20, and a lesser effect on Nrf2 expression was exerted by DMAPT. Reduction of Nrf2 results in the transcriptional decrease of oxidative stress response genes, suggesting that ROS were not removed immediately and instead accumulated within cells (44). In contrast, the present study showed that DMAPT-D6 significantly upregulated the expression of the Nrf2 transcriptional activator. Thus, the results of the present study conflict with the previous study regarding changes in expression levels of Nrf2. Hypothetically, although Nrf2 was significantly upregulated in the present study, resulting in an increase in expression of genes to counteract the increased oxidative stress, this was insufficient in removing the excess ROS due to the potency of DMAPT-D6 on induction of oxidative stress compared with PTL. Moreover, PTL may reduce Nrf2 levels through enhanced ubiquitination and degradation of the Nrf2 protein by Keap1, a factor that mediates ubiquitination and the consequent proteasomal degradation of Nrf2 (44-46). However, the exact mechanism by which the drug increased ROS levels in U87 and LN229 cells requires further study.

It has been reported that γH2AX, (phosphorylated histone H2AX) is a marker of DNA double-strand breaks that accumulates in the nucleus (47). Consistent with this, γH2AX expression was enhanced in the nucleus in a dose-dependent manner in the present study, indicating that DNA damage was significantly induced by upregulation of intracellular ROS. Since DNA damage signaling is a major pathway for induction of cell cycle arrest, it was hypothesized that cell cycle arrest would be induced following treatment with DMAPT-D6 in response to DNA damage (48,49). The results showed that the U87 and LN229 cells were arrested at S-phase induced by DMAPT-D6 treatment, and that S-phase-related proteins were involved in this progression.

Apoptosis, which is initiated by two major pathways, the death-receptor-mediated extrinsic pathway and the mitochondrial-induced intrinsic pathway (50-52), is abnormally regulated in various cancer types, and regarded as a major defense mechanism against tumorigenesis (53,54). Numerous anticancer agents exhibit their inhibitory effects by promoting apoptosis (50-52). Production of caspase-8 induced by the extrinsic pathway can eventually activate caspase 3 which is able to cleave the downstream cellular substrates such as PARP, resulting in progression of apoptosis (55,56). Evidence has shown that certain pharmaceutical compounds cause apoptosis through DNA damage via induction of intracellular ROS (57-59). In agreement with these previous studies, the results of the present study showed that DMAPT-D6 significantly upregulated death receptor signaling pathway-related proteins, such as DR3, DR5, FADD, TRADD and active forms of caspases-3, caspases-8 and PARP, suggesting that death-receptor-mediated extrinsic apoptosis was induced in response to DMAPT-D6 treatment. Based on these data, it was hypothesized that DMAPT-D6 exerted its anticancer effects on GBM cells by inducing extrinsic apoptosis following treatment, and this was due to intracellular accumulation of ROS and the subsequent induction of DNA damage.

In summary, a series of PTL derivatives were synthesized using pharmaceutical methods, and a novel inhibitor with inhibitory effects on GBM cells was identified and termed DMAPT-D6. In DMAPT-D6, hydrogen was substituted for its isotope deuterium in the dimethylamino group. Interestingly, DMAPT-D6 promoted cell cycle arrest at S-phase and cell death-receptor-mediated extrinsic apoptosis pathway due to DNA damage caused by intracellular accumulation of ROS which was induced following treatment with DMAPT-D6. Therefore, the study provides evidence for the use of DMAPT-D6 as an anti-GBM therapy. Future studies should assess the efficacy and value of DMAPT-D6 *in vivo*.

Acknowledgements

Not applicable.

Funding

This research was funded by the Basic Research and Frontier Program of Chongqing Science and Technology Bureau (cstc2018jcyjAX0219, cstc2020jcyj-msxmX0733 and cstc2020jcyj-msxmX0595), Science and Technology Research Program of Chongqing Municipal Education Commission (KJZD-K20200130, KJQN201801304, KJQN201801308 and KJQN201901331) and Scientific Research Foundation of the Chongqing University of Arts and Sciences (2017RBX11, 2017RBX09, Y2020XY14, 2017ZBX05 and 2017ZBX07).

Availability of data and materials

Compounds synthesized in this present study are available from the authors. The datasets used and/or analyzed during the current study are available from the corresponding author on reasonable request.

Authors' contributions

DLY, YL and ZGX conceived and designed the experiments. YJZ, LJH, HXQ and YL conducted the experiments. JHH, YL, DLY and ZGX analyzed and interpreted the data. DYT, ZZC and JHH contributed analysis tools, planned the experiments and participated in the study design and revision process. DLY and YL wrote the paper. All authors read and approved the final manuscript.

Ethics approval and consent to participate

Not applicable.

Patient consent for publication

Not applicable.

Competing interests

The authors declare that they have no competing interests.

References

1. Stupp R, Mason WP, Van Den Bent MJ, Fisher B, Taphoorn MJ, Belanger K, Brandes AA, Marosi C, Bogdahn U, Curschmann J, *et al*: Radiotherapy plus concomitant and adjuvant temozolomide for glioblastoma. New Engl J Med 352: 987-996, 2005.
2. Wen PY and Kesari S: Malignant gliomas in adults. New Engl J Med 359: 492-507, 2008.
3. Ostrom QT, Gittleman H, Xu J, Kromer C, Wolinsky Y, Kruchko C and Barnholtz-Sloan JS: CBTRUS statistical report: Primary brain and other central nervous system tumors diagnosed in the United States in 2009–2013. Neuro Oncol 18: v1-v75, 2016.
4. Louis DN, Ohgaki H, Wiestler OD, Cavenee WK, Burger PC, Jouvet A, Scheithauer BW and Kleihues P: The 2007 WHO classification of tumours of the central nervous system. Acta Neuropathol 114: 97-109, 2007.
5. Wang B, Wu ZS and Wu Q: CMIP promotes proliferation and metastasis in human glioma. Biomed Res Int 2017: 5340160, 2017.
6. Commoner B, Townsend J and Pake GE: Free radicals in biological materials. Nature 174: 689-691, 1954.
7. Sies H: Oxidative stress: Oxidants and antioxidants. Exp Physiol 82: 291-295, 1997.
8. Perry JJ, Shin DS, Getzoff ED and Tainer JA: The structural biochemistry of the superoxide dismutases. Biochim Biophys Acta 1804: 245-262, 2010.
9. Meitzler JL, Antony S, Wu Y, Juhasz A, Liu H, Jiang G, Lu J, Roy K and Doroshow JH: NADPH oxidases: A perspective on reactive oxygen species production in tumor biology. Antioxid Redox Sign 20: 2873-2889, 2014.
10. Fransen M, Nordgren M, Wang B and Apanasets O: Role of peroxisomes in ROS/RNS-metabolism: Implications for human disease. Biochim Biophys Acta 1822: 1363-1373, 2012.
11. Martin KR and Barrett JC: Reactive oxygen species as double-edged swords in cellular processes: Low-Dose cell signaling versus high-dose toxicity. Hum Exp Toxicol 21: 71-75, 2002.
12. Trachootham D, Alexandre J and Huang P: Targeting cancer cells by ROS-mediated mechanisms: A radical therapeutic approach? Nat Rev Drug Discov 8: 579-591, 2009.
13. Fruehauf JP and Meyskens FL Jr: Reactive oxygen species: A breath of life or death? Clin Cancer Res 13: 789-794, 2007.
14. Schumacker PT: Reactive oxygen species in cancer: A dance with the devil. Cancer Cell 27: 156-157, 2015.
15. Tasdogan A, Kumar S, Allies G, Bausinger J, Beckel F, Hofemeister H, Mulaw M, Madan V, Scharffetter-Kochanek K, Feuring-Buske M, *et al*: DNA damage-induced HSPC malfunction depends on ROS accumulation downstream of IFN-1 signaling and bid mobilization. Cell Stem Cell 19: 752-767, 2016.
16. Rodriguez-Rocha H, Garcia-Garcia A, Panayiotidis MI and Franco R: DNA damage and autophagy. Mut Res 711: 158-166, 2011.
17. Knight DW: Feverfew: Chemistry and biological activity. Nat Prod Rep 12: 271-276, 1995.
18. Sun J, Zhang C, Bao YL, Wu Y, Chen ZL, Yu CL, Huang YX, Sun Y, Zheng LH, Wang X and Li YX: Parthenolide-Induced apoptosis, autophagy and suppression of proliferation in HepG2 cells. Asian Pac J Cancer Prev 15: 4897-4902, 2014.
19. Carlisi D, D'Anneo A, Martinez R, Emanuele S, Buttitta G, Di Fiore R, Vento R, Tesoriere G and Lauricella M: The oxygen radicals involved in the toxicity induced by parthenolide in MDA-MB-231 cells. Oncol Rep 32: 167-172, 2014.
20. Al-Fatlawi AA, Al-Fatlawi AA, Irshad M, Rahisuddin and Ahmad A: Effect of parthenolide on growth and apoptosis regulatory genes of human cancer cell lines. Pharm Biol 53: 104-109, 2015.
21. Lu C, Wang W, Jia Y, Liu X, Tong Z and Li B: Inhibition of AMPK/autophagy potentiates parthenolide-induced apoptosis in human breast cancer cells. J Cell Biochem 115: 1458-1466, 2014.
22. Yu HJ, Jung JY, Jeong JH, Cho SD and Lee JS: Induction of apoptosis by parthenolide in human oral cancer cell lines and tumor xenografts. Oral Oncol 51: 602-609, 2015.
23. Zhang S, Ong CN and Shen HM: Critical roles of intracellular thiols and calcium in parthenolide-induced apoptosis in human colorectal cancer cells. Cancer Lett 208: 143-153, 2004.
24. D'Anneo A, Carlisi D, Lauricella M, Emanuele S, Di Fiore R, Vento R and Tesoriere G: Parthenolide induces caspase-independent and AIF-mediated cell death in human osteosarcoma and melanoma cells. J Cell Physiol 228: 952-967, 2013.
25. Liu JW, Cai MX, Xin Y, Wu QS, Ma J, Yang P, Xie HY and Huang DS: Parthenolide induces proliferation inhibition and apoptosis of pancreatic cancer cells in vitro. J Exp Clin Canc Res 29: 108, 2010.
26. Sun Y, St Clair DK, Xu Y, Crooks PA and St Clair WH: A NADPH oxidase–dependent redox signaling pathway mediates the selective radiosensitization effect of parthenolide in prostate cancer cells. Cancer Res 70: 2880-2890, 2010.
27. Anderson KN and Bejcek BE: Parthenolide induces apoptosis in glioblastomas without affecting NF-kappaB. J Pharmacol Sci 106: 318-320, 2008.
28. Guzman ML, Rossi RM, Karnischky L, Li X, Peterson DR, Howard DS and Jordan CT: The sesquiterpene lactone parthenolide induces apoptosis of human acute myelogenous leukemia stem and progenitor cells. Blood 105: 4163-4169, 2005.
29. Nasim S and Crooks PA: Antileukemic activity of aminoparthenolide analogs. Bioorg Med Chem Lett 18: 3870-3873, 2008.
30. Zhang Q, Lu Y, Ding Y, Zhai J, Ji Q, Ma W, Yang M, Fan H, Long J, Tong Z, *et al*: Guaianolide sesquiterpene lactones, a source to discover agents that selectively inhibit acute myelogenous leukemia stem and progenitor cells. J Med Chem 55: 8757-8769, 2012.
31. Long J, Ding YH, Wang PP, Zhang Q and Chen Y: Protection-Group-Free semisyntheses of parthenolide and its cyclopropyl analogue. J Org Chem 78: 10512-10518, 2013.
32. Srinivas US, Tan BW, Vellayappan BA and Jeyasekharan AD: ROS and the DNA damage response in cancer. Redox Biol 25: 101084, 2019.
33. Czarny P, Pawlowska E, Bialkowska-Warzecha J, Kaarniranta K and Blasiak J: Autophagy in DNA damage response. Int J Mol Sci 16: 2641-2662, 2015.
34. Ichijo H, Nishida E, Irie K, ten Dijke P, Saitoh M, Moriguchi T, Takagi M, Matsumoto K, Miyazono K and Gotoh Y: Induction of apoptosis by ASK1, a mammalian MAPKKK that activates SAPK/JNK and p38 signaling pathways. Science 275: 90-94, 1997.
35. Moon DO, Kim MO, Choi YH, Hyun JW, Chang WY and Kim GY: Butein induces G(2)/M phase arrest and apoptosis in human hepatoma cancer cells through ROS generation. Cancer Lett 288: 204-213, 2010.
36. Pelicano H, Feng L, Zhou Y, Carew JS, Hileman EO, Plunkett W, Keating MJ and Huang P: Inhibition of mitochondrial respiration a novel strategy to enhance drug-induced apoptosis in human leukemia cells by a reactive oxygen species-mediated mechanism. J Biol Chem 278: 37832-37839, 2003.
37. Gorrini C, Harris IS and Mak TW: Modulation of oxidative stress as an anticancer strategy. Nat Rev Drug Discov 12: 931-947, 2013.
38. Hou J, Deng Q, Zhou J, Zou J, Zhang Y, Tan P, Zhang W and Cui H: CSN6 controls the proliferation and metastasis of glioblastoma by CHIP-mediated degradation of EGFR. Oncogene 23: 1134-1144, 2017.
39. Li Q, Lu XH, de Wang C, Cai L, Lu JL, Wu JS, Zhuge QC, Zheng WM and Su ZP: Antiproliferative and apoptosis-inducing activity of schisandrin B against human glioma cells. Cancer Cell Int 15: 12, 2015.
40. Ghantous A, Sinjab A, Herceg Z and Darwiche N: Parthenolide: From plant shoots to cancer roots. Drug Discov Today 18: 894-905, 2013.
41. Yang Z, Kuang B, Kang N, Ding Y, Ge W, Lian L, Gao Y, Wei Y, Chen Y and Zhang Q: Synthesis and anti-acute myeloid leukemia activity of C-14 modified parthenolide derivatives. Eur J Med Chem 127: 296-304, 2017.
42. Neelakantan S, Nasim S, Guzman ML, Jordan CT and Crooks PA: Aminoparthenolides as novel anti-leukemic agents: Discovery of the NF-kappaB inhibitor, DMAPT (LC-1). Bioorg Med Chem Lett 19: 4346-4349, 2009.
43. Timmins GS: Deuterated drugs: Where are we now? Expert Opin Ther Pat 24: 1067-1075, 2014.
44. Carlisi D, Buttitta G, Di Fiore R, Scerri C, Drago-Ferrante R, Vento R and Tesoriere G: Parthenolide and DMAPT exert cytotoxic effects on breast cancer stem-like cells by inducing oxidative stress, mitochondrial dysfunction and necrosis. Cell Death Dis 7: e2194, 2016.
45. Cullinan SB, Gordan JD, Jin J, Harper JW and Diehl JA: The Keap1-BTB protein is an adaptor that bridges Nrf2 to a cul3-based E3 ligase: Oxidative stress sensing by a Cul3-Keap1 ligase. Mol Cell Biol 24: 8477-8486, 2004.
46. Ren D, Villeneuve NF, Jiang T, Wu T, Lau A, Toppin HA and Zhang DD: Brusatol enhances the efficacy of chemotherapy by inhibiting the Nrf2-mediated defense mechanism. Proc Natl Acad Sci USA 108: 1433-1438, 2011.

47. Bonner WM, Redon CE, Dickey JS, Nakamura AJ, Sedelnikova OA, Solier S and Pommier Y: GammaH2AX and cancer. Nat Rev Cancer 8: 957-967, 2008.
48. Luo YR, Zhou ST, Yang L, Liu YP, Jiang SY, Dawuli Y, Hou YX, Zhou TX and Yang ZB: Porcine epidemic diarrhoea virus induces cell-cycle arrest through the DNA damage-signalling pathway. J Vet Res 64: 25-32, 2020.
49. Feng Y, Huang H, Gao J and Liu S: Salinomycin induces cell cycle arrest of glioma growth through ROS-mediated DNA damage and AKT inactivation. ACTA Medica Mediterr 36: 249-253, 2020.
50. Huang C, Lu CK, Tu MC, Chang JH, Chen YJ, Tu YH and Huang HC: Polyphenol-Rich avicennia marinaleaf extracts induce apoptosis in human breast and liver cancer cells and in a nude mouse xenograft model. Oncotarget 7: 35874-35893, 2016.
51. Hilliard T, Miklossy G, Chock C, Yue P, Williams P and Turkson J: 15α-methoxypuupehenol induces antitumor effects *in vitro* and *in vivo* against human glioblastoma and breast cancer models. Mol Cancer Ther 16: 601-613, 2017.
52. Nayak VL, Nagesh N, Ravikumar A, Bagul C, Vishnuvardhan MV, Srinivasulu V and Kama A: 2-Aryl benzimidazole conjugate induced apoptosis in human breast cancer MCF-7 cells through caspase independent pathway. Apoptosis 22: 118-134, 2017.
53. Xiang M, Su H, Shu G, Wan D, He F, Loaec M, Ding Y, Li J, Dovat S, Yang G and Song C: Amplexicaule A exerts anti-tumor effects by inducing apoptosis in human breast cancer. Oncotarget 7: 18521-18530, 2016.
54. Gao L, Wang Y, Xu Z, Li X, Wu J, Liu S, Chu P, Sun Z, Sun B, Lin Y, *et al*: SZC017, a novel oleanolic acid derivative, induces apoptosis and autophagy in human breast cancer cells. Apoptosis 20: 1636-1650, 2015.
55. Hamzeloo-Moghadam M, Aghaei M, Fallahian F, Jafari SM, Dolati M, Abdolmohammadi MH, Hajiahmadi S and Esmaeili S: Britannin, a sesquiterpene lactone, inhibits proliferation and induces apoptosis through the mitochondrial signaling pathway in human breast cancer cells. Tumour Biol 36: 1191-1198, 2015.
56. Cheng YC, Hueng DY, Huang HY, Chen JY and Chen Y: Magnolol and honokiol exert a synergistic anti-tumor effect through autophagy and apoptosis in human glioblastomas. Oncotarget 7: 29116-29130, 2016.
57. Hang W, Yin ZX, Liu G, Zeng Q, Shen XF, Sun QH, Li DD, Jian YP, Zhang YH, Wang YS, *et al*: Piperlongumine and p53-reactivator APR-246 selectively induce cell death in HNSCC by targeting GSTP1. Oncogene 37: 3384-3398, 2018.
58. Yang Y, Zhang Y, Wang L and Lee S: Levistolide A induces apoptosis via ROS-mediated ER stress pathway in colon cancer cells. Cell Physiol Biochem 42: 929-938, 2017.
59. Colin D, Limagne E, Ragot K, Lizard G, Ghiringhelli F, Solary É, Chauffert B, Latruffe N and Delmas D: The role of reactive oxygen species and subsequent DNA-damage response in the emergence of resistance towards resveratrol in colon cancer models. Cell Death Dis 5: e1533, 2014.